PHYSICAL REVIEW B

CONDENSED MATTER

THIRD SERIES, VOLUME 49, NUMBER 6 1 FEBRUARY 1994-II

Near-edge sodium and fluorine K-shell photoabsorption of alkali halides

E. Hudson and E. Moler
Department of Chemistry, University of California, Berkeley, California 94720
and Chemical Sciences Division, Lawrence Berkeley Laboratory, University of California, Berkeley, California 94720

Y. Zheng
Chemical Sciences Division, Lawrence Berkeley Laboratory, University of California, Berkeley, California 94720
and Departments of Chemistry and Physics, Pennsylvania State University, University Park, Pennsylvania 16802

S. Kellar
Department of Chemistry, University of California, Berkeley, California, 94720
and Chemical Sciences Division, Lawrence Berkeley Laboratory, University of California, Berkeley, California 94720

P. Heimann and Z. Hussain
Accelerator and Fusion Research Division, Lawrence Berkeley Laboratory, University of California, Berkeley, California 94720

D. A. Shirley
Departments of Chemistry and Physics, Pennsylvania State University, University Park, Pennsylvania 16802
(Received 2 September 1993)

The x-ray-absorption near-edge structure (XANES) spectra of single-crystal alkali halide salts have been measured at low temperature ($T \approx 80$ K) with high resolution in energy. By employing the electron partial-yield detection technique, spectra of NaF, NaCl, and NaBr were obtained near the sodium K edge and spectra of LiF, NaF, and KF were obtained near the fluorine K edge. All spectra showed sharp absorption features at the absorption threshold and broader features extending 50–80 eV above threshold. Some narrow features close to threshold are attributed to core-level excitons. Contributions from atomic multiple-electron excitations, estimated by a comparison to the K-edge photoabsorption spectrum of Ne in the gas phase, are found to be very small. Thus, the intense broader peaks observed further above threshold arise from single-electron scattering resonances. These highly structured spectra of well-characterized ordered crystals provide a set of standard data which is used to test the multiple-scattering x-ray-absorption code FEFF V. For some spectra, at photon energies more than ≈ 10 eV above threshold, the calculations achieve very good agreement with experiment. The dependence of the calculation on cluster size, order of scattering, and choice of self-energy is demonstrated.

I. INTRODUCTION

X-ray-absorption near-edge structure (XANES) is used to study local electronic and geometric structure, in particular, to characterize the bonding geometry and valence of selected elements in a compound or complex.[1–4] In recent years, theoretical advances, partly motivated by the needs of extended x-ray-absorption fine-structure (EXAFS), have provided a more quantitative understanding of XANES spectra.[5–10] It is important to test the predictions of the improved theory by comparison to measured XANES spectra of relatively well-characterized systems. The structural parameters of alkali halide crystals have been known for some time, in particular their crystal structures, lattice constants, and Debye temperatures. The XANES spectra of these compounds contain very sharp fine structure close to the edges and fairly intense resonances extending well above the absorption thresholds, thus providing good test cases for theoretical simulations.

In this work, K-edge XANES spectra were measured for a number of single-crystal alkali halides. The combination of high resolution in energy and low sample temperature allowed the detection of extensive fine structure from below threshold to ≈ 60–90 eV above the edge. The observed structure is attributed to core-level excitons very near the edge and photoelectron scattering resonances further above the edge. The spectra provide a set of standard data, which is compared to curved-wave multiple-scattering simulations generated by the FEFF

0163-1829/94/49(6)/3701(8)/$06.00

code, developed by Rehr, Albers, and co-workers.[5,6,11] For several spectra, the FEFF simulations give very good agreement with the experimental results, at photon energies more than ≈ 10 eV above threshold. A comparison of simulations demonstrates that multiple scattering and distant scatterers (>7 Å from emitter in some cases) must be included in the calculation to obtain the best agreement with experiment. The choice of photoelectron self-energy used in the calculation shows a notable effect on the results.

II. EXPERIMENTAL DETAILS

XANES spectra were obtained with high resolution in energy using soft x rays from the Lawrence Berkeley Laboratory Spherical Grating Monochromator on Beam Line 6-1 at the Stanford Synchrotron Radiation Laboratory. Photoabsorption spectra of NaF, NaCl, and NaBr were measured near the sodium K edge using the second and third orders of diffraction with an estimated spectral resolution of 0.5 eV. Spectra of LiF, NaF, and KF were measured near the fluorine K edge using the first order of diffraction with an estimated spectral resolution of 0.3 eV. The single crystals were cleaved along the (100) face in the vacuum chamber at pressures of $\approx 5\times 10^{-10}$ Torr. XANES spectra near the oxygen K edge detected no oxygen on the cleaved samples, indicating that the crystals were not hydrated. Spectra were measured at temperatures near 80 K. Absorption of x rays by the samples was detected by measuring the partial electron yield with a channeltron. Although this detection technique does not directly measure photoabsorption, partial-yield spectra are generally very similar to corresponding photoabsorption spectra. The retardation potential of the detector was selected to accept the Auger electrons corresponding to the core level of interest, even in the event of sample charging. Some spectra were measured, while using a beam of low-energy electrons from a flood gun to neutralize the surface charge, but no charging-related effects were observed.

III. EXPERIMENTAL RESULTS

A. Overview

The Na K-edge XANES spectra of NaF, NaCl, and NaBr at $T\approx 80$ K are shown in Fig. 1. These spectra agree with earlier measurements made over a narrower energy range at room temperature using polycrystalline films.[4] The NaCl spectrum was also measured previously at low temperature,[12] with sharp near-edge structure very similar to that shown here. Figure 2 shows the F K-edge spectra of LiF, NaF, and KF measured at $T\approx 80$ K. Similar spectra were previously measured on single crystals over a narrower energy range at an unspecified temperature.[13]

For spectra at the Na K edge of NaF and NaBr and at the F K edge of NaF, the relative orientation of the x-ray linear-polarization vector and the crystal axes were varied. Spectra obtained with the polarization vector aligned along the [100], [110], and [111] crystallographic directions were virtually identical. For all the spectra shown in Figs. 1 and 2, the [110] axis was parallel to the x-ray polarization vector.

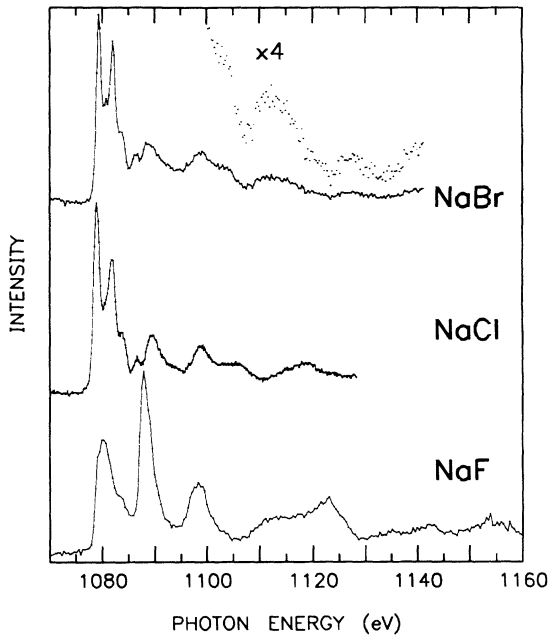

FIG. 1. Photoabsorption spectra of sodium halide salts near the sodium K edge. For NaBr, weaker absorption features are also shown with an expanded vertical scale.

X rays are known to induce defect formation in alkali halide crystals.[14] No evidence of radiation damage was observed in this experiment, however. As a test, Na K-edge spectra of NaBr were measured on a previously

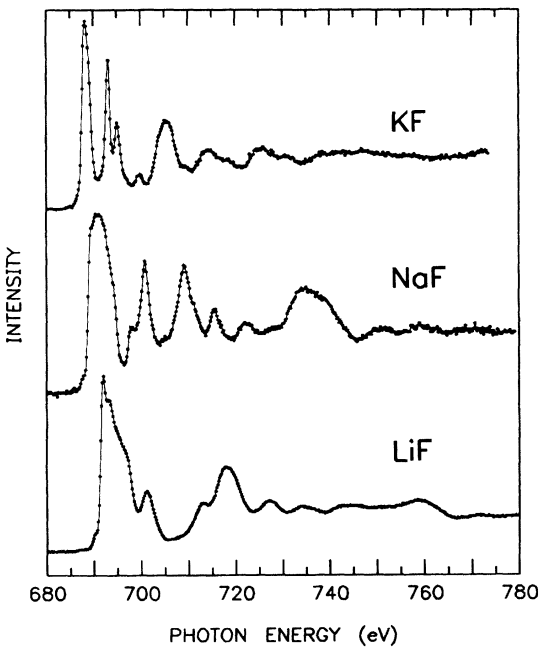

FIG. 2. Photoabsorption spectra of alkali fluoride salts near the fluorine K edge.

unirradiated surface with the minimum possible photon flux and exposure time. The spectrum obtained was the same as spectra measured after prolonged exposures to x rays.

B. Discussion

All of the spectra in Figs. 1 and 2 show sharp absorption features near threshold and broader resonances extending 60–90 eV above threshold. The narrow lines below and possibly just above threshold are attributed to core-level excitons, i.e., the excitation of the core electron into a bound state just below the conduction band.[15] These excitons are not easily identified in the spectra, however, because the exact energy of the ionization threshold is generally not known. Broader above-threshold peaks are attributed to photoelectron scattering resonances. These prominent features are observed when a single electron is promoted to a continuum state, which is resonantly enhanced at the absorber by single and multiple scattering from the surrounding ions. The distinction between excitons and photoelectron scattering resonances is, in effect, mainly that of bound vs unbound electron states; in both cases the presence of the core hole may strongly influence the final states[15] and multiple-scattering theory can be used to model the final states.[13,16]

In general, fine structure above absorption edges may also be produced by multiple-electron excitations. Such features are the result of the simultaneous promotion of a core electron and one or more valence electrons to bound and/or free final states. These "shake up" and "shake off" excitations are observed in many systems but are generally much less intense, relative to the edge jump, than the features observed here.[2,17] For comparison purposes, the K edge spectrum of Ne gas was measured with high resolution using the SX700/II monochromator at BESSY.[18] Atomic Ne is isoelectronic to Na^+ and F^- ions. Figure 3 compares the K-edge spectra for Ne gas and for sodium and fluorine in NaF, aligned at the lowest-energy inflection points. The Ne spectrum shows weak, narrow peaks at $\approx$35–45 and 58 eV, which are attributed to multiple-electron excitations.[19] However, the combined intensity of these features is only a very small fraction of the total area under the step associated with the absorption edge. This result indicates that contributions from multiple-electron excitations will be very weak in the alkali halide XANES spectra presented here.

As mentioned above, some spectra were measured with different orientations of the x-ray polarization vector with respect to the crystal lattice. The spectral features showed no dependence upon this change in experimental geometry. Such a dependence might be expected, in particular, for the features closest to the absorption edge because of the well-defined spatial symmetries of similar XANES resonances in free and adsorbed molecules.[20] The lack of a polarization effect suggests that the excited states observed in each individual spectrum share the same or similar spatial symmetries.

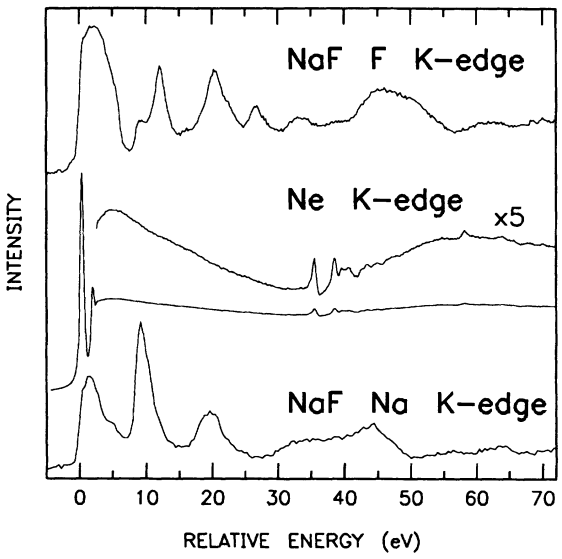

FIG. 3. Comparison of the K-edge spectra of sodium and fluorine in NaF with that of neon. The above-edge structure in the Ne spectrum, also shown with an expanded vertical scale, arises from multiple-electron excitations. The spectra are aligned at their lowest-energy inflection points, which are 688.6 eV, 869.3 eV, and 1078.7 eV for NaF (F K edge), Ne, and NaF (Na K edge), respectively.

IV. SIMULATIONS USING FEFF V

A. Choice of parameters

The curved-wave electron scattering code FEFF developed by Rehr, Albers, and co-workers allows the calculation of extended x-ray-absorption fine-structure (EXAFS) spectra.[5,6] A recently released version (FEFF V) also includes contributions from multiple-scattering paths, which become more important at lower electron energies.[11] This is currently the best available version for the modeling of XANES spectra at energies above threshold. Simulations using FEFF V (version 5.05) have been performed for all spectra presented here. Because the properties of alkali halide crystals are well-known, structural parameters were not varied in the simulations. Several nonstructural aspects of the calculations were varied to establish their relative contributions and to characterize the origins of the observed spectral features. In several cases, the simulations are quite successful in modeling the measured spectra at photon energies more than $\approx$10 eV above threshold. Results indicate noticeable contributions from distant scatterers and multiple scattering. The choice of photoelectron self-energy has a significant effect upon the results.

Parameters for the simulations were selected to best model the known experimental conditions. Each compound studied has the NaCl crystal structure. Lattice constants for each crystal were interpolated from tables in Ref. 21 for the measurement temperatures. Debye temperatures were taken from Ref. 22. FEFF V cannot presently model polarized x-ray absorption. Although the experiment used linearly polarized x rays, the as-

sumption of unpolarized radiation for the simulation should not effect the results appreciably, in light of the complete absence of observed angular effects described above. FEFF calculations do not provide the absolute photon energy of the ionization threshold, so the threshold energy must be estimated by comparison to experimental results. Because of the possibility of pre-edge transitions, it is nontrivial to determine the threshold energy from the measured spectrum. For each of the comparisons shown here, the ionization threshold energy for the measured spectrum was chosen to best fit the simulation.

The partial electron yield technique used to monitor the absorption of x-rays by the sample is somewhat surface-sensitive. The measured signal arises mainly from those Auger electrons which retain most of their kinetic energy as they propagate from the emitter to the vacuum. The effective sensitivity depth is thus determined by the mean free path of the Auger electron. At the Na and F *KLL* Auger energies, the mean free path is predicted by FEFF to be 30–60 Å for the crystals studied. This indicates that the present measurements are dominated by bulk absorbers and that surface effects have little influence on the experimental results. Furthermore, test simulations using FEFF predict only minor differences between the spectra of bulk and surface absorbers. When the absorber was placed on or near an unreconstructed surface, only a general decrease in the amplitude of the simulation was observed, with no distortion of the features, as compared to a bulk absorber. The simulations presented here were calculated for a bulk absorber, i.e., no surface was modeled in the cluster. In all the calculations, except as noted below, the largest practical cluster size (389 atoms, 18 shells) was used, thereby maximizing the likelihood of a converged simulation.

B. Self-energy of the photoelectron

One difficulty in the modeling of near-edge spectra is the limited accuracy of the available self-energies for the photoelectron in the low-kinetic-energy region. In the formulation used by FEFF, the self-energy is a local potential, which is added to the Coulomb potential of the photoelectron.[23] The real part of the self-energy approximates the exchange-correlation potential of the photoelectron. An imaginary part of the self-energy can be used to model the inelastic energy losses, i.e., the extrinsic losses which determine the mean free path of the photoelectron. In previous comparisons, both the Dirac-Hara[24] (DH) and Hedin-Lundqvist[25] (HL) self-energies have had some success in the simulation of XANES (Ref. 26) and EXAFS (Refs. 6, 23, 27, and 28). The DH self-energy has no imaginary part, and thus does not model mean-free-path effects, whereas the HL self-energy includes an energy-dependent imaginary part, which models the inelastic losses of the photoelectron. Both self-energies include an energy dependence in the real part.

In Figs. 4 and 5, the results of FEFF simulations using the DH and HL self-energies are compared to the χ curves extracted from the data using a standard EXAFS-like analysis.[29] In this analysis, the extrapolated pre-edge background was subtracted from the data, a spline fit to the result was used to normalize the curve, and unity was then subtracted to give $\chi(E)$, the experimental χ curve. Overall, the simulations of the spectra give fairly good agreement with the experimental χ curves at energies more than 5–10 eV above threshold. Especially success-

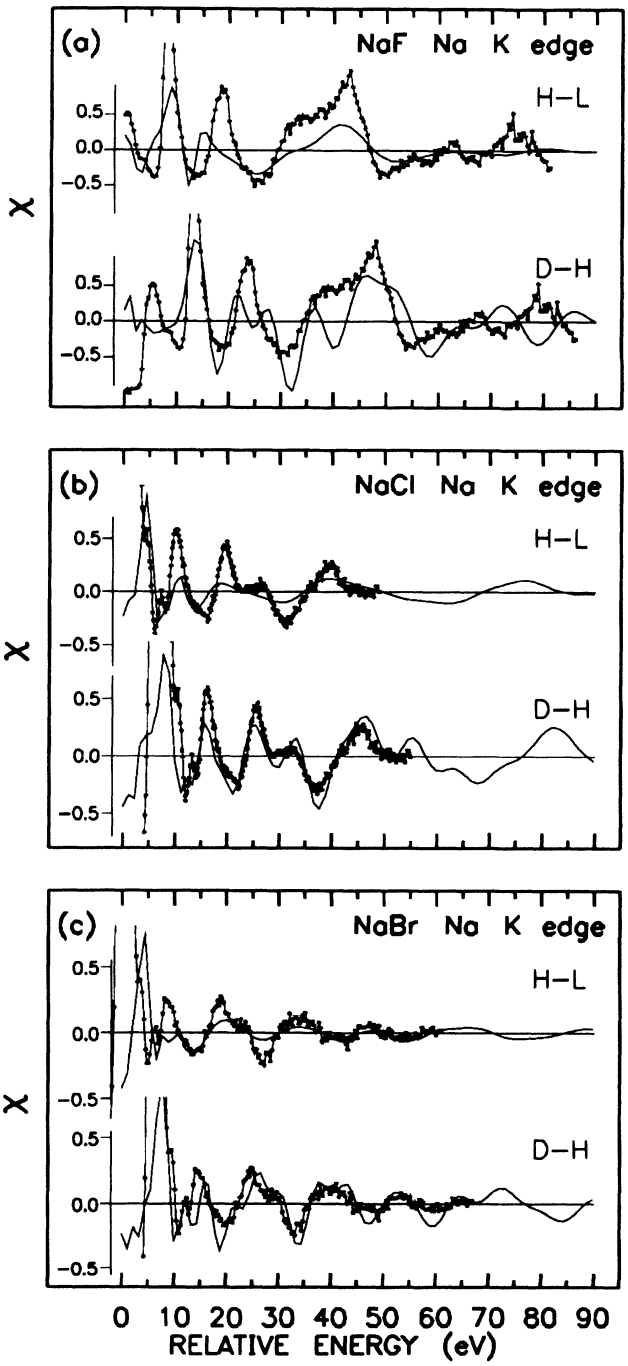

FIG. 4. Comparison of experimental (dotted lines) and calculated (solid lines) XANES spectra of sodium halides at the Na *K* edge. In each panel, simulations using the HL and DH self-energies are compared to experimental spectra. For each comparison, the zero of energy for the experimental spectrum is chosen to give the best agreement with the simulation. (a) NaF results. (b) NaCl results. (c) NaBr results.

ful simulations are obtained for the spectra of NaCl and NaBr, and for the lower-energy portion of the LiF spectrum.

The HL simulations have smaller amplitudes than in the corresponding DH simulations; this is expected because the DH self-energy does not include photoelectron attenuation. In contrast, the HL potential appears to overestimate the photoelectron inelastic losses, as shown in Figs. 4 and 5 by the predicted amplitudes, which are consistently smaller than the experimental results. These amplitude errors are larger than those commonly found using FEFF with the HL self-energy.[30] Disagreements between experimental results and the DH simulations are seen mainly for the lower-frequency features, whereas the HL simulations model higher-frequency oscillations less successfully. These trends are seen as the absence of narrower features in some HL simulations [especially for the F K edges (Fig. 5)] and as offset peak positions in the low- and high-energy parts of some DH simulations [particularly for NaF, Figs. 4(a) and 5(b)]. Figure 6 illustrates these results for the NaF F K-edge spectra by comparing the Fourier transforms (FT's) of the data and simulations of Fig. 5(b). The path length for the first peak in the experimental FT is reproduced slightly better in the HL FT than in the DH FT. The features at somewhat larger path lengths ($\approx$6–13 Å) are modeled better by the DH FT, both in magnitude and position. The DH FT gives too much magnitude at the largest path lengths shown ($>$13 Å), probably because the mean free path is overestimated (see below). These results indicate that the HL self-energy gives a mean free path which is too short at near-edge energies, thereby underestimating the contributions from distant scatterers. The HL self-energy presumably matches the lower-frequency components better because it provides, in the real part, a more accurate model of the energy dependence of the self-energy. This is consistent with the results for transition metals in Ref. 6, obtained by comparing measured and calculated scattering phases, which show the HL self-energy to be more accurate than the DH self-energy.

The present results do not clearly favor either self-energy considered here. In the LiF spectra of Fig. 5(a),

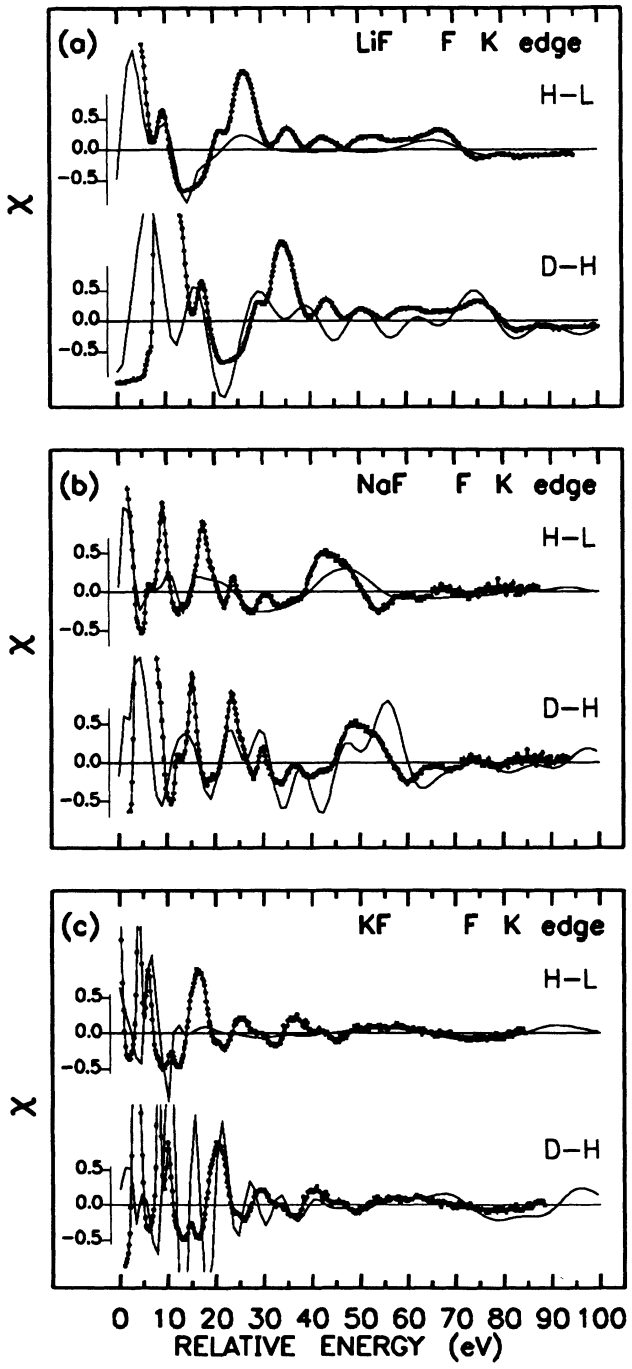

FIG. 5. Comparison of experimental (dotted lines) and calculated (solid lines) XANES spectra of alkali fluorides at the F K edge. See Fig. 4 caption for details. (a) LiF results. (b) NaF results. (c) KF results.

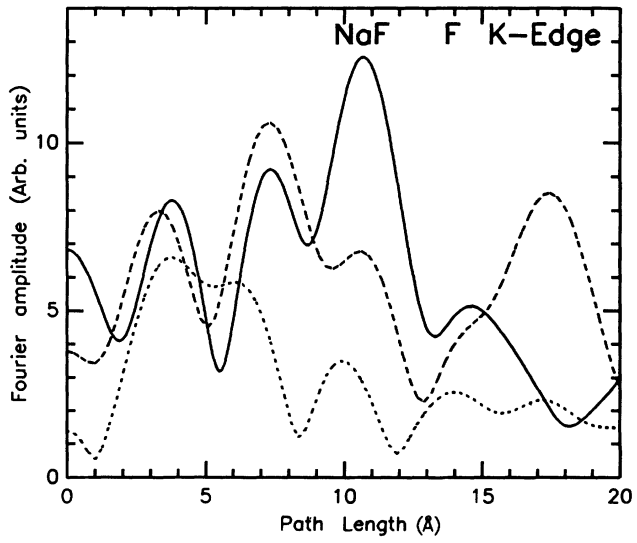

FIG. 6. Fourier transforms of NaF F K-edge XANES spectra: experimental (solid line); simulation using HL self-energy (short-dashed line); simulation using DH self-energy (long-dashed line). Spectra were converted from an energy scale to a photoelectron momentum scale before transformation; thus the FT ordinate represents scattering path length. To convert the experimental spectrum, the ionization threshold was assumed to be 691 eV, which is the value used for the comparison to the HL simulation in Fig. 5(b).

for example, the lower-energy range is modeled quite well by the HL simulation, while in the higher-energy range the DH model is somewhat better. For NaCl [Fig. 4(b)], the DH simulation clearly gives a better shape and amplitude than the HL simulation. However, a previous comparison of the NaCl Na K edge spectrum to scattering calculations based on smaller clusters concluded that the HL model is slightly better.[26] It seems that neither self-energy is completely sufficient for general use in the calculation of alkali halide XANES spectra, and improved models are required. The present results suggest that the main limitation of the HL self-energy is in the imaginary part, and that a better model of inelastic losses might lead to significantly improved simulations.

All the simulations shown here assume the correlated Debye model for the calculation of Debye-Waller factors, which may underestimate the effective thermal disorder for distant scatterers. The DH calculations tend to overestimate contributions from large path lengths, as shown by the FT results for NaF (see Fig. 6). Of course, this may result simply from an overestimate of the photoelectron mean free path. But a better treatment of thermal disorder in the calculation could also reduce the amplitude contributed by those paths which include distant scatterers. Thus, in the present study it is difficult to separate the effects of mean free path and thermal disorder. However, as more reliable near-edge self-energies are developed, temperature-dependent measurements of the alkali halide XANES spectra could be used to characterize the thermal disorder of scatterers well outside the first few coordination shells.

C. Cluster-size and scattering-order dependence

At kinetic energies below $\approx 15-20$ eV the electron mean free path becomes very large, particularly in insulators at energies less than that of the band gap. The XANES spectrum just above threshold can include contributions from long scattering paths and thus may be affected by scatterers well outside the first few coordination shells. It is therefore important to evaluate the effects of cluster size on the simulations. Figures 7 and 8 show the cluster-size dependence for simulations of the LiF and NaBr spectra. In these comparisons, the maximum scattering path length, $R_{\max}$, was limited to twice the radius of the 18-shell cluster, except as noted otherwise. By comparing panels (a) and (b) in Figs. 7 and 8, it is seen that increasing the cluster radius from 6.9 to 9.0 Å in LiF and from 10.3 to 13.3 Å in NaBr (i.e., increasing from 11 to 18 shells) gives an improved agreement with experiment for the first ≈ 15 eV above threshold. These results demonstrate that even distant scatterers can contribute to the lower-energy XANES of alkali halides.

It has been known for some time that multiple-scattering (MS) calculations are necessary to adequately describe XANES spectra in a variety of systems.[11,31] Therefore the simulations shown in Figs. 4 and 5 include higher-order contributions; up to fifth-order MS (i.e., six-legged paths) for NaF and LiF, and up to seventh-order MS for the higher-Z compounds. These cutoffs were indirectly determined in the calculation by limiting the total scattering path length, $R_{\max}$, and by filtering out

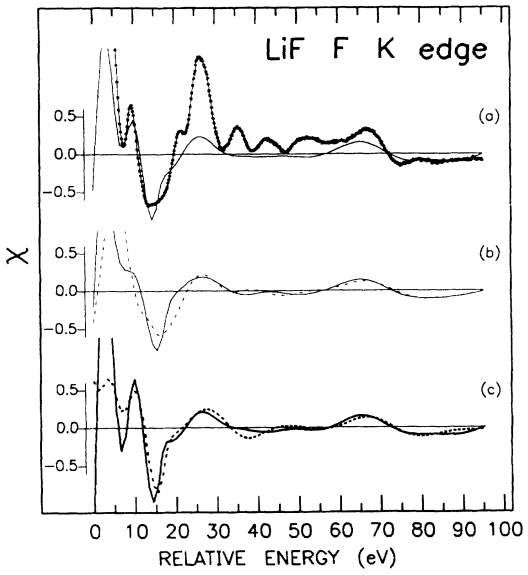

FIG. 7. Dependence of simulations upon cluster size and scattering order of the LiF F K edge XANES. All calculations shown use the HL self-energy. (a) Comparison of experimental results (dotted line) and calculation (solid line) using an 18-shell cluster and full multiple scattering (MS) [as shown in Fig. 5(a)]. (b) Simulations using an 11-shell cluster (solid line) and a four-shell cluster (dashed line). (c) Simulations using an 18-shell cluster with up to three orders of MS (solid line) and with single-scattering only (dashed line). The agreement with data in the lower-energy range improves significantly when the cluster size is increased from 11 to 18 shells.

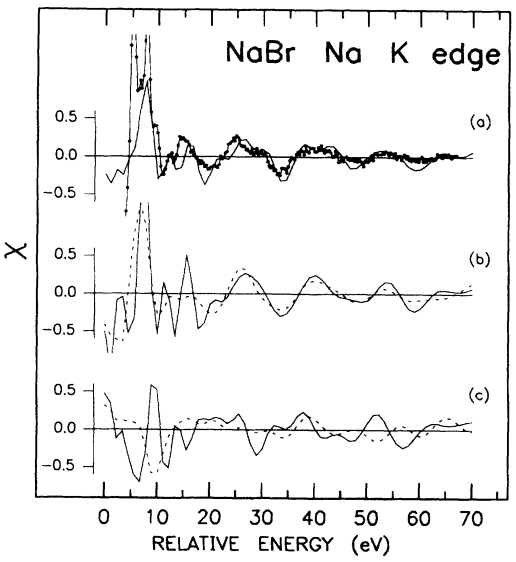

FIG. 8. Dependence of simulations upon cluster size and scattering order for the NaBr Na K-edge XANES. All calculations shown use the DH self-energy. (a) Comparison of experimental results (dotted line) and calculation (solid line) using an 18-shell cluster and full multiple scattering (MS) [as shown in Fig. 4(c)]. (b) Simulations using an 11-shell cluster (solid line) and a four-shell cluster (dashed line). (c) Simulations using an 18-shell cluster with up to three orders of MS (solid line) and with single scattering only (dashed line). The agreement with data in the lower-energy range improves significantly when the MS is increased from third to seventh order.

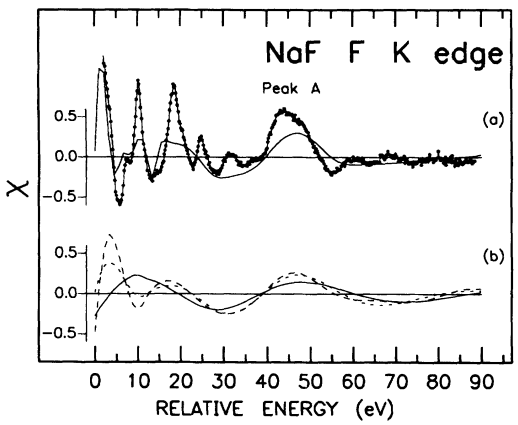

FIG. 9. Dependence of simulations upon cluster size and maximum path length for the NaF F K-edge XANES. All calculations shown use the HL self-energy. (a) Comparison of experimental results (dotted line) and calculated (solid line) using an 18-shell cluster [as shown in Fig. 5(a)]. (b) Simulations using a one-shell cluster with single scattering (SS) (solid line); a two-shell cluster with SS (short-dashed line); and a two-shell cluster with multiple scattering (R_{max} = twice the 18-shell cluster radius) (long-dashed line). Note that the peak at ≈45 eV in the data is approximately reproduced even by the two-shell SS calculation.

those paths which produced very weak amplitudes at the emitter. Figures 7(c) and 8(c) show the effects of limiting the scattering order. These results clearly demonstrate the importance of higher-order contributions to the simulations, especially in the lower-energy XANES region. However, limiting the calculation to third-order MS (i.e., up to four-legged paths) gives nearly the same results as the full-order simulation for most of the present spectra.

The prominent feature at ≈45 eV in the NaF F K-edge spectrum [peak A in Fig. 9(a)] is of particular interest because it is unusual to see such an intense peak in the higher part of the XANES energy range. The FEFF simulations in this energy range are nearly converged even for very small clusters and single scattering (SS), as shown in Fig. 9. In fact, a calculation with only seven atoms (a one-shell cluster) already shows a broad feature at the correct energy. The one-shell SS result shown in Fig. 9(b) was almost identical to a one-shell MS calculation (not shown). Increasing the cluster size to 19 atoms (two shells) gives a narrower, more intense resonance at ≈45 eV, which is nearly converged to the 18-shell MS result shown in Fig. 9(a). For the two-shell cluster, the MS simulation of peak A is only slightly narrower than in the SS simulation. These results suggests a simpler interpretation for peak A than for most of the observed XANES structure. The near-convergence of this feature in the SS simulation with the two-shell cluster indicates that it is best described as an intense low-energy EXAFS feature. Because of its large intensity and proximity to threshold, peak A might be likened to a molecular shape resonance, e.g., the well-known above-edge MS resonances in SF_6.[32] The present work shows that the peak arises predominantly from SS, however, indicating that the shape-resonance view is inadequate in this case.

The experimental Na K-edge spectrum of NaF shows a fairly intense feature centered at ≈35 eV. Calculations using small clusters (not shown) give results somewhat similar to those found for the NaF F K edge: a resonance near the correct energy is obtained even for the simplest simulations. In this case, however, the two-shell simulations are not as close to the 18-shell result as they are for the F K edge, and the improvement going from SS to MS is notable in the two-shell simulations. These results suggest that, in NaF, the resonance ≈35 eV above the Na K edge is not as simple to interpret as the corresponding resonance, peak A, ≈40 eV above the F K edge.

V. CONCLUSIONS

The fluorine and sodium K-edge XANES for a series of alkali halides has been measured at low temperature using single crystals cleaved *in vacuo*. The results provide a set of standard spectra, which were used to test the recently developed multiple-scattering FEFF V code. For several compounds, there is very good agreement between calculated and measured spectra. The comparison of calculations based on the Hedin-Lundqvist and Dirac-Hara self-energies shows that neither self-energy is completely reliable and that improvements to the HL model of inelastic losses are needed. For some compounds, scatterers more than 7 Å from the emitter influence the XANES spectra for energies less than ≈15 eV. In general, multiple scattering is found to greatly influence the XANES spectra. A notable exception is the ≈45-eV resonance above the F K edge for NaF, which is best described as an unusually intense single-scattering EXAFS peak.

ACKNOWLEDGMENTS

We thank M. Domke for measuring the Ne photoabsorption spectrum at our request, and J. Rehr and S. Zabinsky for help in the use of FEFF and for valuable discussions. This work was supported by the Director, Office of Energy Research, Office of Basic Energy Sciences, Chemical Sciences Division of the U.S. Department of Energy under Contract No. DE-AC03-76SF00098.

[1] *EXAFS and Near Edge Structure,* Springer Series in Chemical Physics, Vol. 27, edited by A. Bianconi, L. Incoccia, and S. Stipcich (Springer-Verlag, Berlin, 1983).

[2] A. Bianconi, in *X-Ray Absorption: Principles, Applications, Techniques of EXAFS, SEXAFS, and XANES,* edited by D. C. Koningsberger and R. Prins (Wiley, New York, 1988).

[3] For examples, see J. Petiau, G. Calas, and P. Sainctavit, J. Phys. (Paris) Colloq. **48**, C9-1085 (1987); W. Gädeke, E. E. Koch, G. Dräger, R. Frahm, and V. Saile, Chem. Phys. **124**, 113 (1988); J. Evans and J. F. W. Mosselmans, J. Phys. Chem. **95**, 9673 (1991); N. Thromat, C. Noguera, M. Gautier, F. Jollet, and J. P. Duraud, Phys. Rev. B **44**, 7904 (1991).

[4] T. Fujikawa, T. Okazawa, K. Yamasaki, J. Tang, T. Murata, T. Matsukawa, and S. Naoé, J. Phys. Soc. Jpn. **58**, 2952 (1989);

T. Murata, T. Matsukawa, and S. Naoé, Physica B **158**, 610 (1989).

[5]J. J. Rehr, J. Mustre de Leon, S. I. Zabinsky, and R. C. Albers, J. Am. Chem. Soc. **113**, 5135 (1991).

[6]J. Mustre de Leon, J. J. Rehr, S. I. Zabinsky, and R. C. Albers, Phys. Rev. B **44**, 4146 (1991).

[7]L. Fonda, J. Phys. Condens. Matter **4**, 8269 (1992).

[8]T. Fujikawa, T. Matsuura, and H. Kuroda, J. Phys. Soc. Jpn. **52**, 905 (1983).

[9]A. Bianconi, A. DiCiccio, N. V. Pavel, M. Benfatto, A. Marcelli, C. R. Natoli, P. Pianetta, and J. Woicik, Phys. Rev. B **36**, 6426 (1987).

[10]J. E. Müller and J. W. Wilkins, Phys. Rev. B **29**, 4331 (1984).

[11]J. J. Rehr, R. C. Albers, and S. I. Zabinsky, Phys. Rev. Lett. **69**, 3397 (1992).

[12]T. Murata, T. Matsukawa, and S. Naoé, Solid State Commun. **66**, 787 (1988).

[13]S. Nakai, M. Ohashi, T. Mitsuishi, H. Maezawa, H. Oizumi, and T. Fujikawa, J. Phys. Soc. Jpn. **55**, 2436 (1986).

[14]See, e.g., F. C. Brown, B. R. Sever, N. Kristianpoller, and J. P. Stott, Phys. Scr. **35**, 582 (1987).

[15]S. Pantelides, Phys. Rev. B **11**, 2391 (1975).

[16]I. I. Gegusin, V. N. Datsyuk, A. A. Novakovich, L. A. Bugaev, and R. V. Vedrinskii, Phys. Status Solidi B **134**, 641 (1986).

[17]A. Bianconi, J. Garcia, M. Benfatto, A. Marcelli, C. R. Natoli, and M. F. Ruiz-Lopez, Phys. Rev. B **43**, 6885 (1991), and references therein.

[18]For a description of the monochromator see M. Domke, T. Mandel, A. Puschmann, C. Xue, D. A. Shirley, G. Kaindl, H. Petersen, and P. Kuske, Rev. Sci. Instrum. **63**, 80 (1992).

[19]J. M. Esteva, B. Gauthé, P. Dhez, and R. C. Karnatak, J. Phys. B **16**, L263 (1983).

[20]W. H. E. Schwarz, Angew. Chem. Internat. Edit. **13**, 454 (1974); J. Stöhr and R. Jaeger, Phys. Rev. B **26**, 4111 (1982).

[21]W. Pies and A. Weiss, *Crystal Structure Data of Inorganic Compounds,* Landolt-Börnstein, Neue Serie, Gruppe III, Band 7, Teil a, edited by K.-H. Hellwege and A. M. Hellwege (Springer-Verlag, Berlin, 1973).

[22]J. T. Lewis, A. Lehoczky, and C. V. Briscoe, Phys. Rev. **161**, 877 (1967).

[23]S.-H. Chou, J. J. Rehr, E. A. Stern, and E. R. Davidson, Phys. Rev. B **35**, 2604 (1987).

[24]S. Hara, J. Phys. Soc. Jpn. **22**, 710 (1967); P. A. M. Dirac, Proc. Cambridge Philos. Soc. **26**, 376 (1930).

[25]Hedin and Lundqvist, Solid State Phys. **23**, 1 (1969).

[26]R. Gunella, M. Benfatto, A. Marcelli, and C. R. Natoli, Solid State Commun. **76**, 109 (1990).

[27]T. A. Tyson, M. Benfatto, C. R. Natoli, B. Hedman, and K. O. Hodgson, Physica B **158**, 425 (1989).

[28]R. F. Pettifer and A. D. Cox, in *EXAFS and Near Edge Structure,* edited by A. Bianconi, L. Incoccia, and S. Stipcich (Springer-Verlag, Berlin, 1983), p. 66.

[29]P. A. Lee, P. H. Citrin, P. Eisenberger, and B. M. Kincaid, Rev. Mod. Phys. **53**, 769 (1981).

[30]D. Lu and J. J. Rehr, Phys. Rev. B **37**, 6126 (1988).

[31]J. Dehmer and D. Dill, Phys. Rev. Lett. **35**, 213 (1975); C. A. Ashley and S. Doniach, Phys. Rev. B **11**, 1279 (1975); F. W. Kutzler, C. R. Natoli, D. K. Misemer, S. Doniach, and K. Hodgson, J. Chem. Phys. **73**, 3274 (1980); P. J. Durham, J. B. Pendry, and C. H. Hodges, Solid State Commun. **38**, 159 (1981).

[32]T. A. Tyson, K. O. Hodgson, C. R. Natoli, and M. Benfatto, Phys. Rev. B **46**, 5997 (1992).